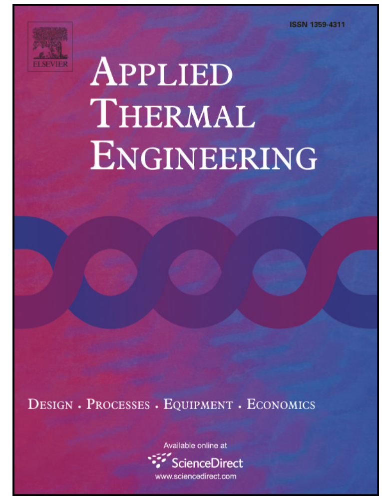

Research Paper

The effect of temperature dependent relative permeability on heavy oil recovery during hot water injection process using streamline-based simulation

Mohammad Hossein Doranehgard, Majid Siavashi

PII: S1359-4311(17)33517-2
DOI: https://doi.org/10.1016/j.applthermaleng.2017.10.002
Reference: ATE 11200

To appear in: *Applied Thermal Engineering*

Received Date: 24 May 2017
Revised Date: 2 September 2017
Accepted Date: 2 October 2017

The effect of temperature dependent relative permeability on heavy oil recovery during hot water injection process using streamline-based simulation

---

Mohammad Hossein Doranehgard
Master of Science
Applied Multi-Phase Fluid Dynamics Lab., School of Mechanical Engineering, Iran University of Science and Technology, Iran.
Email: m_doraneh@mecheng.iust.ac.ir

Majid Siavashi (Corresponding author):
Assistant Professor
Applied Multi-Phase Fluid Dynamics Lab., School of Mechanical Engineering, Iran University of Science and Technology, Iran

Email: msiavashi@iust.ac.ir
Postal address: School of Mechanical Engineering, Iran University of Science and Technology, Narmak, Tehran, Iran. Postal Code: 1684613114.
Telephone: +98 21 77240391.
Fax: +98 21 77240488.

September 2017

The effect of temperature dependent relative permeability on heavy oil recovery during hot water injection process using streamline-based simulation

Mohammad Hossein Doranehgard[a], **Majid Siavashi**[a*]

[a] *Applied Multi-Phase Fluid Dynamics Lab., School of Mechanical Engineering, Iran University of Science and Technology*
**Corresponding Author:msiavashi@iust.ac.ir*

Abstract

Extraction of heavy viscous oil from oilfields requires thermal enhanced oil recovery techniques to reduce the oil viscosity and improve its mobility. Usually, in these problems the effects of temperature on the relative permeability are ignored. In this paper, hot water injection into oil reservoirs (3D heterogeneous porous media) with temperature dependent viscosity and relative permeability functions is simulated numerically using an improved streamline approach to enhance computational performance. To this end, pressure and conduction equations are solved simultaneously on a 3D Eulerian grid, and saturation and heat convection equations are solved along multiple 1D streamlines. Results of the old and the modified thermal streamline simulator are compared in terms of the norm of error, and a significant improvement in accuracy of results is observed. Finally, the new numerical simulator employed to investigate effects of temperature dependent relative permeability on oil recovery of four sample heavy oilfields. It has been shown that these effects have a remarkable impact on the efficiency of hot water injection process and large errors can be caused, ignoring relative permeability changes with temperature in realistic reservoirs.

Keywords: Hot water injection, thermal enhanced oil recovery, relative permeability, heavy oil reservoir, porous media, streamline simulation.

Nomenclature

c_j	Compressibility of j th phase (kPa^{-1})	S_{wc}	Water connate saturation
C_r	Specific heat capacity ($kJ.\ kg^{-1}.K^{-1}$)	T	Temperature (K)
E	Energy per unit volume ($kJ.m^{-3}$)	$\mathbf{u}_j$	Darcy velocity of j th phase ($m.s^{-1}$)
f_j	Fractional flow of j th phase	U_j	Specific energy of j th phase per unit mass ($kJ.kg^{-1}$)
G_T	Energy transfer by gravity effects ($kJ.\ m^{-2}.s^{-1}$)	V_p	Pore volume of the grid cell
G_w	Mass transfer by gravity effects ($kg.\ m^{-2}.s^{-1}$)		
H_j	Special enthalpy of j th phase per unit mass ($kJ.\ kg^{-1}$)	***Greek symbols***	
$\mathbf{k}$	Permeability (m^2)	α_t	Thermal expansion coefficient (K^{-1})
k_r	Thermal conductivity of rock ($Wm^{-1}K^{-1}$)	Δt_{sl}	Local timestep on a streamline (s)
k_{rj}	Relative permeability of j th phase	$\Delta\tau$	Time-of-flight difference (s)
K_T	Total thermal conductivity ($Wm^{-1}K^{-1}$)	ϕ	Porosity
$\dot{m}_j$	Mass flow rate of j th phase per unit of volume ($kg.m^{-3}s^{-1}$)	λ_j	Mobility of j the phase
p	Pressure (kPa)	μ	Viscosity (Pa. s)
q_t	Total flow rate per unit of volume (s^{-1})	ρ_j	Density of j th phase ($kg.m^{-3}$)
q_H	Total heat source (Wm^{-3})	ρ_r	Density of rock phase ($kg.m^{-3}$)
S_j	j th phase saturation	τ	Time-of-flight (s)
S_{or}	*Oil residual saturation*		

1. Introduction

According to available statistics, more than 68 percent of the world's proven oil resources are heavy oil [1]. As a consequence of high viscosity and density of heavy oil compared to light oil, heavy oil requires thermal EOR processes to increase its mobility and extract it from rock layers [2]. Nowadays, the use of numerical techniques is the most important tool to simulate hydrocarbon reservoirs to gain a proper understanding from behavior of fluid flow and heat transfer within reservoirs. The streamline-based simulation method, in comparison with the traditional numerical schemes, can substantially decrease the simulation time and reduce the required computational memory of computers. Furthermore, this method provides a good visualization of flow, presents the inter-connection between wells properly, can be parallelized easily, and introduces new engineering information for engineers [3].

The streamline-based simulation method, with the key feature that fluid transport occurs on a streamline grid rather than between gridblocks, was first introduced by Batycky et al. [4] and employed to simulate the water injection process (waterflooding) in a 3D field-scale reservoir. Afterward, this technique has been developed rapidly so that it becomes a complete simulator for complex fluid flow simulation in different oilfields such as compressible flow [5], fractured reservoirs [6][7], compositional flow [8], polymer injection [9-12] and well placement [13]. Interested researchers can find more details and an extensive literature survey about theory and development of streamline-based simulation technique in the reference [3].

A few studies have also been carried out to develop the streamline-base method to simulate thermal EOR processes. The first study performed by Pasarai and Arihara [14] in a 2D reservoir with an injector and a producer without gravity and conduction heat transfer effects. They suggested to solve the energy equation along streamlines, as well as the saturation equation. They concluded that additional research is required to improve the numerical solution of mass and energy transport equations along streamlines. Zhu et al. [15] more extensively illustrated this method to simulate hot water injection in two-dimensional reservoir models considering gravity and conduction effects. They solved the advective part of the mass and energy equations along streamlines, and then accounted the gravity and conduction effects on the 3D underlying grid. They also studied the accuracy of this method of solution for different Peclet numbers (convection to conduction ratios) and concluded that this method could provide reasonable results. Siavashi et al. [16] extended the streamline-based simulation to hot water injection in 3D and tested their numerical solver in the SPE-10 reservoir model with multiple wells. They also investigated the effect of global time-steps and the number of streamlines on performance and accuracy of the streamline method.

According to the literature, in all the previous research studies on simulation of thermal EOR processes by the streamline simulation technique, oil viscosity was changing moderately with temperature and the relative permeability was considered independent of temperature. While, some investigations about the effect of temperature on relative permeability reported that a significant difference has been observed between results of the case with temperature dependent relative permeability in comparison with cases in which relative permeability are considered independent from temperature [17-25]. Since the streamline method decouples the governing equations and solves them separately, the accuracy of the method might be weakened by increasing the non-linearity of governing equations, caused by variations of the relative permeability and the oil viscosity. Accordingly, the aim of this research is to improve the streamline-based simulation method to simulate hot water injection process to enhance oil recovery from heavy oilfields with an acceptable accuracy, taking into account the relative permeability as a function of temperature with a higher range of oil viscosity variations. In addition, the SPE-10 model – a 3D highly heterogeneous reservoir model with fine-scale grids including more than 1 million cells – is used to study the performance of the streamline simulator in 3D. Finally, effects of temperature dependent relative permeability on the recovery of reservoirs are investigated in four sample oilfields. It will be shown that the streamline technique can provide appropriate results with an improved performance. In addition, it has been concluded that temperature effects on relative permeability have a high impact on oil production of heavy oilfields and have to be considered in thermal EOR studies.

2. Mathematical modeling and governing equations

This study assumes that oil and water pressure are always higher than their bubble pressure, and therefore the flow is two-phase and no gas phase exists in the reservoir. In addition, it is supposed that oil and water are immiscible and their components are present only in their phases. All fluid phases are considered to be in thermal equilibrium with rocks and the kinetic energy of fluid is also considered to be negligible. In addition, it is assumed that porous media are saturated with two phases of oil and water. For simplicity, the effect of capillary pressure is also neglected. Therefore, mass conservation equation for water and oil phases can be written as follows:

$$\frac{\partial\left(\phi\rho_j S_j\right)}{\partial t}+\nabla\cdot\left(\rho_j \mathbf{u}_j\right)=\dot{m}_j \qquad j=w,o \tag{1}$$

where ϕ, ρ_j and S_j represent the porosity, density and saturation of j th phase, respectively. $\dot{m}_j$ represents the mass flow rate of j th phase per unit of volume. $\mathbf{u}_j$ is Darcy velocity of j th phase expressed by Darcy's law [26]:

$$\mathbf{u}_j=-\mathbf{k}\frac{k_{rj}}{\mu_j}.\left(\nabla p_j+\rho_j g\nabla D\right) \tag{2}$$

In Eq. (2), p_j, μ_j and k_{rj} are the phase pressure, the viscosity and the relative permeability of j th phase, respectively. $\mathbf{k}$ is the absolute permeability of porous rocks and D is the depth.

Since the porous media are saturated with fluid phases:

$$\sum_{j=w,o} S_j=1 \tag{3}$$

To calculate the temperature, the energy conservation equation can be written as follows [26, 27]:

$$\frac{\partial E}{\partial t}+\nabla.\left(\sum_{j=w,o}\rho_j\mathbf{u}_j H_j\right)-\nabla.\left(K_T\nabla T\right)=q_H \tag{4}$$

E is given by:

$$E=\phi\sum_{j=w,o}\rho_j S_j U_j+(1-\phi)\rho_r C_r T \tag{5}$$

By inserting Darcy equation (2) in mass conservation equation (1) and doing some algebraic operations [16], the pressure equation can be obtained as follows :

$$\phi c_t \frac{\partial P}{\partial t}-\phi\alpha_t\frac{\partial T}{\partial t}-\sum_{j=w,o}\frac{1}{\rho_j}\nabla.(\rho_j \mathbf{u}_j)=q_T \tag{6}$$

In the above equation, the total compressibility is defined as $c_t=\sum_{j=w,o}c_j S_j$. It should be noted that in this study the compressibility of the rock has been ignored. In addition, since no gas phase exists in the reservoir the liquid phases are assumed to be approximately incompressible (c_j=10^{-7} kPa^{-1}).

3. Streamline-based simulation technique

Before description of different steps of streamline-based simulation, it's necessary to define time-of-flight (TOF) parameter and represent the saturation and energy equations in terms of TOF. Afterward, the streamline-based solution procedure is described in section 3.2.

3.1 Time-of-flight (TOF)

Time-of-flight (τ) is defined as the time taken for a neutral tracer to travel the specific distance of s along a streamline, and is expressed as follows:

$$\tau=\int_0^s\frac{\phi(\zeta)}{\left|\mathbf{u}_\mathbf{t}(\zeta)\right|}d\zeta \tag{7}$$

By some algebraic manipulations this definition of TOF can lead to the following operator:

$$\left|\mathbf{u}_\mathbf{t}(\zeta)\right|\frac{\partial}{\partial\zeta}=\mathbf{u}_\mathbf{t}\cdot\nabla=\phi\frac{\partial}{\partial\tau} \tag{8}$$

Implementing the above operator in the mass and energy equations, assuming the gravity acts in-line with the z-coordinate, they can be represented in terms of TOF as follows [16]:

$$\frac{\partial M_w}{\partial t}+\frac{\partial F_w}{\partial \tau}+\frac{1}{\phi}\frac{\partial G_w}{\partial z}=0 \tag{9}$$

$$\frac{\partial}{\partial t}\left(E/\phi\right)+\frac{\partial F_H}{\partial \tau}+\frac{1}{\phi}\frac{\partial G_T}{\partial z}-\frac{1}{\phi}\nabla.\left(k_T\nabla T\right)=0 \tag{10}$$

where $M_w=\rho_w S_w$, $F_w=\rho_w f_w$ and $F_H=\sum_{j=w,o}\rho_j f_j H_j$. G_w and G_T are respectively the mass and energy transfer terms due to gravity effects, and are given by:

$$G_w=k_z\rho_w\frac{\lambda_w\lambda_o}{\lambda_t}\left(\rho_w-\rho_o\right)g \tag{11}$$

$$G_T=k_z\frac{\lambda_w\lambda_o}{\lambda_t}\left(\rho_w H_w-\rho_o H_o\right)\left(\rho_w-\rho_o\right)g \tag{12}$$

k_z is the rock permeability in z-direction, λ_w and λ_o are the mobility of water and oil phases respectively, and $\lambda_t=\lambda_w+\lambda_o$ is the total mobility.

To solve Eqs. (9) and (10), the operator splitting technique is used and they are solved in three separate steps, using results of their previous step as the initial condition. First, the heat conduction term of the energy equation (10), i.e. Eq. (13), is solved with the pressure equation for a global timestep, as described in section 3.2.

$$\frac{\partial}{\partial t}\left(E/\phi\right)-\frac{1}{\phi}\nabla.\left(k_T\nabla T\right)=0 \tag{13}$$

The advective parts of the mass and energy equations (Eq. (14)) are solved along streamlines.

$$\begin{cases}\dfrac{\partial M_w}{\partial t}+\dfrac{\partial F_w}{\partial \tau}=0\\[2mm]\dfrac{\partial}{\partial t}\left(E/\phi\right)+\dfrac{\partial F_H}{\partial \tau}=0\end{cases} \tag{14}$$

Energy and mass variations due to the gravity are solved along gravity lines which are in line with the z coordinate, using Eq. (15).

$$\begin{cases}\dfrac{\partial M_w}{\partial t}+\dfrac{1}{\phi}\dfrac{\partial G_w}{\partial z}=0\\[2mm]\dfrac{\partial}{\partial t}\left(E/\phi\right)+\dfrac{1}{\phi}\dfrac{\partial G_T}{\partial z}=0\end{cases} \tag{15}$$

3.2 Solution procedure

For reservoir simulation by streamlines – unlike other conventional methods – three grids and three time grids are required. The spatial grids involve: 1- a 3D Eulerian computational grid in the reservoir space; 2- several 1D grids on streamlines; and 3- several 1D grids along the gravity vector. The three time grids are: 1- global timesteps or pressure timesteps that are used to update the pressure field on the 3D underlying Eulerian grid; 2- local timesteps or transport timesteps used to solve the saturation and energy equations on multiple 1D streamline grids; and 3- the local timesteps to solve the saturation and energy equations along gravity lines. In Fig. 1, the mentioned timestep grids and their relationship are exhibited.

Fig. 1 Schematic of timestep grids in the streamline-based method.

In Fig. 2, different steps of the thermal streamline-based technique for simulation of hot waterflooding process in hydrocarbon reservoirs are briefly described. It is worthy to mention that this method is applicable for, incompressible (or slightly compressible) flows and for compressible flows a different solution procedure to solve transport equations along streamlines is demanded [5]. As is shown in Fig. 2, after initialization of parameters the global timestep is selected. In the streamline simulation technique, like IMPES method, the pressure equation and mass and energy transport equations are solved separately. Initially, it is assumed that the saturation is constant and by definition of the reservoir geometry, boundary conditions, well locations and the initial condition of the reservoir, the pressure equation can be discretized and solved on the 3D Eulerian grid using an implicit solver. Using the second order central difference scheme, the discretized form of the pressure Eq. (6) could be written as follows:

$$
\begin{aligned}
&\frac{\left(V_p c_t\right)_{i,j,k}}{\Delta t_p}\left(P_{i,j,k}^{n+1}-P_{i,j,k}^{n}\right)-\frac{\left(\alpha_t V_p \Delta T\right)_{i,j,k}}{\Delta t_p} \\
&-\left(TX\right)_{i+1/2}\left(P_{i+1,j,k}^{n+1}-P_{i,j,k}^{n+1}\right)+\left(TX\right)_{i-1/2}\left(P_{i,j,k}^{n+1}-P_{i-1,j,k}^{n+1}\right) \\
&-\left(TY\right)_{j+1/2}\left(P_{i,j+1,k}^{n+1}-P_{i,j,k}^{n+1}\right)+\left(TY\right)_{j-1/2}\left(P_{i,j,k}^{n+1}-P_{i,j-1,k}^{n+1}\right) \\
&-\left(TZ\right)_{k+1/2}\left(P_{i,j,k+1}^{n+1}-P_{i,j,k}^{n+1}\right)+\left(TZ\right)_{k-1/2}\left(P_{i,j,k}^{n+1}-P_{i,j,k-1}^{n+1}\right) \\
&+\left(G\right)_{k+1/2}\left(z_{i,j,k+1}-z_{i,j,k}\right)-\left(G\right)_{k-1/2}\left(z_{i,j,k}-z_{i,j,k-1}\right)=\left(Q_w+Q_o\right)_{i,j,k}=\left(Q_T\right)_{i,j,k}
\end{aligned}
\tag{16}
$$

where TX, TY and TZ are the total transmissibility in x, y and z directions, respectively. G is also the total gravity transmissibility.

In the present study, in order to better handle non-linearity effects, a modification is suggested in this step, and the heat conduction equation is solved simultaneous with the pressure equation in a coupled system of equations. Hence, temperature variation effects due to conductive heat transfer on the pressure equation can be accounted in this step. Temperature variations caused by convection will be accounted in another step.

The heat conduction Eq. (13) can also be discretized and represented by:

$$
\begin{aligned}
&\frac{\left(V_p\right)_{i,j,k}}{\Delta t_p}\left(\left(E/\phi\right)_{i,j,k}^{n+1*}-\left(E/\phi\right)_{i,j,k}^{n}\right) \\
&-KX_{i+1/2}\left(T_{i+1}^{n+1*}-T_{i,j,k}^{n+1*}\right)+KX_{i-1/2}\left(T_{i,j,k}^{n+1*}-T_{i-1}^{n+1*}\right) \\
&-KY_{j+1/2}\left(T_{j+1}^{n+1*}-T_{i,j,k}^{n+1*}\right)+KY_{j-1/2}\left(T_{i,j,k}^{n+1*}-T_{j-1}^{n+1*}\right) \\
&-KZ_{k+1/2}\left(T_{k+1}^{n+1*}-T_{i,j,k}^{n+1*}\right)+KZ_{k-1/2}\left(T_{i,j,k}^{n+1*}-T_{k-1}^{n+1*}\right)=0
\end{aligned}
\tag{17}
$$

KX, KY and KZ are respectively the conductive heat fluxes in x, y and z directions. In the above equations, superscript n+1 stands for the next global timestep, and n+1* indicates the updated temperature values in the next global timestep with only conductive heat transfer effects.

Since, temperature variations caused by non-conductive heat transfer terms might lead to significant errors in the pressure equation, consequently ΔT in Eq. (16) is estimated as follows:

$$\Delta T_{i,j,k} = \left(T_{i,j,k}^{n+1*} - T_{i,j,k}^{n}\right) + \left(\Delta T_{i,j,k}^{n}\right)_{\text{non-cond.}} \tag{18}$$

where $\left(\Delta T_{i,j,k}^{n}\right)_{\text{non-cond.}}$ is the non-conductive temperature changes in the previous global timestep, and is set to zero in the first global timestep.

Afterward, effects of new pressure and temperature field on transmissibility factors are accounted, and total Darcy velocity is calculated to trace streamlines using Pollock's semi-analytical method [28]. In this step, there are some cells which no streamline has been passed through them. Hence, missed cells are found to trace backward streamlines from these cells toward injection wells. Now, saturation and temperature should be updated by accounting their changes due to fluid flow along streamlines. Accordingly, these parameters are mapped on streamlines to start solution along them. Details about backward tracing of streamlines and also mapping parameters from 3D grid on streamlines and vice versa are available in [16, 29].

Next, the advective part of the mass and energy equations (Eq. (14)) are solved simultaneously on separate streamlines using their specific local time-steps. It's worthy to mention that the same streamlines are implemented to solve the advective part of the mass and energy equations. These equations are discretized using an explicit first order upstream-weighted scheme as follows:

$$\begin{cases} \left(M_w\right)_i^{n+1} = \left(M_w\right)_i^{n} - \dfrac{\Delta t_{sl}}{\Delta \tau}\left(\left(F_w\right)_i - \left(F_w\right)_{i-1}\right) \\ \left(E/\phi\right)_i^{n+1} = \left(E/\phi\right)_i^{n} - \dfrac{\Delta t_{sl}}{\Delta \tau}\left(\left(F_U\right)_i - \left(F_U\right)_{i-1}\right) \end{cases} \tag{19}$$

In the above relations $\Delta\tau$ represents $\left(\tau_i - \tau_{i-1}\right)$, in which τ_i is the TOF to the i th cell. In addition, Δt_{sl} is the local timestep on a streamline and is estimated using the CFL, Courant–Fredrich-Lewy criterion [30] to be confident about stability of the solution. Eq. (19**Error!**

Reference source not found.) is solved until the end of the global timestep, and the updated results will be used as the initial condition for the gravity segregation step.

Fig. 2 Solution diagram of the thermal streamline-based simulation

At the end of a global timestep, results of the previous step are mapped back to the 3D underlying grid, and mass and energy of cells are updated to account for gravity effects using Eq. (15). This equation is discretized and solved in the same manner as the advection equation along streamlines, up to the end of the global timestep. Now, if the solution is reached to the end of simulation time, the solution is terminated, otherwise, the same procedure continues to the end of required simulation time.

4. Problem description

4.1 Fuid properties

The main effect of hot water injection on fluid properties is the viscosity reduction caused by temperature increment. In this study, a heavy oil is used and variation of its viscosity with temperature is exhibited in Fig. 3 [31]. As can be seen, the viscosity of heavy oil at 293K is 140 cp, and by increasing the temperature up to 363 K, its viscosity drops and reach to 40 cp. Fig. 4 also shows the variation of the water viscosity with temperature [32] which is used in the investigated problems.

The density of the fluid phases in terms of temperature and pressure is described by the following equation [32]:

$$\rho_j(T,P)=\rho_j^{ref}\exp\left[c_j\left(p-p_{ref}\right)-\alpha_j\left(T-T_{ref}\right)\right] \tag{20}$$

In the above relation, p_{ref} and T_{ref} are respectively the reference pressure and temperature. ρ_j^{ref} is density of i th phase at the reference temperature and pressure. Constant parameters used in this investigation to define the density of fluid phases are presented in Table 1 [33, 34].

Table 1 Compressibility, thermal expansion coefficient and reference density of fluid phases used in Eq. (20) [33, 34]

fluid	ρ_j^{ref} (kg.m^{-3})	c_j (kPa^{-1})	α_j (K^{-1})
water	998	1×10^{-7}	1×10^{-4}
oil	804.6	1×10^{-7}	1×10^{-4}
T_{ref} = 273 K, P_{ref} = 100 kPa			

Fig. 3 Viscosity variations heavy oil with temperature

Fig. 4 Viscosity variations of the water with temperature

As previously mentioned, no gas phase exists in the reservoir; hence the compressibility values are very low. However, the difference between densities of the oil and water phases is almost high and can better show the capability of the numerical solver for simulation of this problem.

The effective thermal conductivity of the bulk volume containing fluid phases and rock is defined as follows [35]:

$$k_T = (1-\phi)k_r + \phi(S_w k_w + S_o k_o) \quad (21)$$

where k_r, k_w and k_o are the thermal conductivity of rock, water and oil, respectively. The thermal conductivity for the fluid phases and the rock are set to 0.6 Wm^{-1}K^{-1} and 3.5 Wm^{-1}K^{-1}, respectively. To calculate the enthalpy and the internal energy, the following relations are used [36]:

$$H_{L,j} = \left(\overline{C}_{P,L}\right)_j \left(T - T_{ref}\right) \tag{22}$$

$$U_j = H_{L,j} - p / \rho_j \tag{23}$$

where $\left(\overline{C}_{P,L}\right)_j$ is the average thermal capacity of j th phase obtained by integration over a temperature interval. In this study, the thermal capacity of water and oil phases are respectively considered to be 4.19 and 2.02 kJ.kg^{-1}.K^{-1}, and for the rock $\rho_r C_r = 2300$ kJ. m^{-3}.K^{-1} [37].

4.2 Relative permeability

Temperature variations can change the irreducible water saturation (S_{wc}) and also the oil residual saturation (S_{or}). In addition, the contact angle of oil/water and also their interfacial tension can be affected by temperature changes with subsequent wettability alteration. Hence, the relative permeability function in some reservoir rocks has to be considered as a function of temperature. Poston et al. [38] presented data for unconsolidated sandstone rocks and observed an increase in the relative permeability by temperature increase. They also found an increase in S_{wc} and a decrease in S_{or} by temperature increment. They mentioned that unconsolidated sands become more water-wet with an increase in temperature. Miani and Okazawa [39] in their experimental research on silica sandstone rocks pointed out that wettability alteration due to temperature variations changes the relative permeability. They also observed a similar trend for unconsolidated sandstone rocks. Al-Hadhrami and Blunt [40] in a field case study showed that at a transition temperature chalky limestone rocks would undergo through a wettability reversal process from oil-wet to water-wet. Hamouda et al. [17, 20, 41] in a series of research works dealing with chalk/water/oil interactions, observed that with increasing temperature, S_{wc} will be approximately constant, but, the residual oil saturation will be faced with a significant decrease. They showed that increasing the temperature, improves the water wetness of the oil-wet chalk. They also presented a series of calculations on the wettability alteration mechanism at elevated temperatures taking into account the fluid/rock interaction forces and disjoining pressure.

According to the mentioned research studies, the main difference between silica/unconsolidated sandstone rocks and chalk/limestone rocks is that, in chalk/limestone rocks with increasing temperature S_{wc} will be approximately constant, while, for sandstone rocks with ascending temperature, the irreducible water saturation will experience a high increase. As a consequence, with increasing the temperature, it's expected to have more oil production in chalk/limestone reservoirs and lower oil production in sandstone rocks.

In the present study, in order to investigate the effect of temperature on relative permeability and its subsequent effect on oil recovery from reservoirs, different relative permeability functions are employed by the streamline simulator. First, the common Stone's model, which has been employed for simulation of hot waterflooding in the previous studies [15, 16, 42], is used as the base case with a temperature independent relative permeability function. The Stone's model is presented as follows:

$$\begin{aligned} k_{rw} &= \left(\frac{S_w - S_{wc}}{1 - S_{wc} - S_{or}}\right)^2 \\ k_{ro} &= \left[1 - \left(\frac{S_w - S_{wc}}{1 - S_{wc} - S_{or}}\right)\right]^2 \end{aligned} \tag{24}$$

In the above relation, k_{rw} and k_{ro} depend only on water saturation (S_w), and are independent of temperature. S_{wc} and S_{or} are assumed to be constant and equal to 0.22 and 0, respectively [20, 25]. To further study the effect of temperature on relative permeability, four other relative permeability functions are also used which are functions of both the water saturation and temperature [18-20, 23].

According to experimental investigations conducted on chalk hydrocarbon reservoir rocks [17, 20], the relative permeability of water and oil phases can be represented as follows:

$$k_{rw} = \left(\frac{S_w - S_{wc}}{1 - S_{wc}}\right)^{(2+3\alpha)/\alpha}$$
$$k_{ro} = \left[1 - \left(\frac{S_w - S_{wc}}{1 - S_{wc}}\right)\right]^2 \times \left[1 - \left(\frac{S_w - S_{wc}}{1 - S_{wc}}\right)^{(2+\alpha)/\alpha}\right] \tag{25}$$

In Eq. (25), α and S_{wc} are temperature dependent coefficients which can be obtained by experimental investigations. In this work, values of these parameters are selected from the experimental data presented by [17, 20], and are exhibited in Table 2 using linear interpolation. In addition, S_{or} is assumed to be constant and equal to zero [17, 25].

Table 2 Empirical coefficients of Eq. (25) as a function of temperature [17]

T(K)	S_{wc}	α
296	0.2	6.62
323	0.21	5.67
353	0.2	9.835
403	0.17	4.241

The second temperature dependent relative permeability function is considered for a reservoir with limestone rocks. Based on empirical investigations by Sola et al. [21] the following relations are proposed for calculation of the relative permeability in this kind of reservoir rocks:

$$k_{rw} = k_{rw}^{o}(S)^{nw} \qquad 0.4 < nw < 2.0 \qquad 0.25 < k_{rw}^{o} < 0.4$$
$$k_{ro} = k_{ro}^{o}(1-S)^{no} \qquad 0.8 < no < 1.8 \qquad 0.2 < k_{ro}^{o} < 1 \tag{26}$$
$$S = \frac{S_w - S_{wc}}{1 - S_{wc}}$$

where k_{rw}^{o}, k_{ro}^{o}, *no*, *nw* and S_{wc} are empirical coefficients and their values at two different temperatures are shown in Table 3 [21]. The value of these parameters at other temperatures will be calculated by a linear approximation in the presented temperature range.

Table 3 Empirical coefficients of Eq. (26) as a function of temperature [21]

T (K)	no	nw	S_{wc}	k^{o}_{rw}	k^{o}_{ro}
310	1.8	2.0	0.35	0.25	1
366	0.8	0.4	0.35	0.4	0.2

The third temperature dependent relative permeability function is dedicated to the silica sandstones rocks, and are presented according to the empirical research done by Maini and Okazawa [39], as follows:

$$k_{rw} = \frac{(S^*)^{n_w} + 1.01\,S^*}{1.01}$$
$$k_{ro} = \frac{(1-S^*)^{n_o} + 1.01\,(1-S^*)}{1.01} \tag{27}$$
$$S^* = \frac{S_w - S_{wc}}{1-S_{wc}-S_{or}}$$

In which n_w and n_o are empirical temperature dependent powers and are calculated from Table 4, with linear interpolation.

Table 4 Empirical coefficients of Eq. (27) as a function of temperature [39].

T (K)	n_w	n_o
294	1.56	1.99
333	0.625	1.97
373	1.19	3
423	2.3	2.68

The fourth implemented relative permeability function is for unconsolidated sandstone rocks, which is presented based on an empirical study conducted by Poston et al. [38]:

$$k_{rw} = \left(\frac{S_w - S_{wc}}{1-S_{wc}}\right)^2$$
$$k_{ro} = \left[1-\left(\frac{S_w - S_{wc}}{1-S_{wc}}\right)\right]^2 \tag{28}$$

and S_{wc} is obtained from Table 5, using linear interpolation [38].

Table 5 Empirical coefficients of Eq. (28) as a function of temperature [38].

T (K)	S_{wc}
297	0.22
320	0.2
344	0.18
380	0.15

4.3 The reservoir model

In the present study, the SPE-10 reservoir model is used for simulation of hot waterflooding. SPE-10 is a 3D heterogeneous reservoir model organized by the Society of Petroleum Engineers as a comparative solution project to compare the performance of different numerical reservoir simulators. The model is a 365.8×670.6×51.8 m^3 reservoir with a sufficiently fine grid (containing 60×220×85=1.122 million cells) consists of a part of Brent sequence in North Sea.

A vertical injection well exists at the center of the reservoir and hot water at 363 K is injected into the reservoir. In addition, four vertical production wells exist at reservoir corners and are controlled with a constant bottom-hole pressure of 5000 kPa. The radius of all wells is considered as r_w=0.0762 m. The initial pressure and temperature within the reservoir are assumed to be 100 kPa and 293 K, respectively, and the corresponding value of S_{wc} at the initial temperature is considered for the initial water saturation. The porosity and the horizontal distribution of reservoir permeability values in different layers of the reservoir are depicted in Fig. 5 and Fig. 6, respectively.

Fig. 5 Porosity distribution of the SPE-10 model in its different layers.

Fig. 6 Horizontal permeability of the SPE-10 model in its different layers.

5. Results and discussion

In this section, hot waterflooding process of the problem described in the previous section is simulated by the thermal streamline-based simulator and results are presented for different conditions. First, a sensitivity study is performed to study the effect of the new modification made in simulator on error of results. In the next step, effects of temperature dependent relative permeability on oil production rates and volume are investigated for four reservoir models with chalk, limestone, silica sandstone and unconsolidated sandstone rocks.

5.1 Sensitivity study

Results of streamline simulator depend on the number of pressure updates (NPU) and the number of forward streamlines (NSL). In this section, the effect of these parameters on the difference between results of the streamline method and those of the grid-based simulator (as the reference case) is discussed. Since the simulation of the full SPE-10 model is very time consuming, hence an upscaled model with a coarse grid is employed for sensitivity study. Results are compared in terms of L_1 norm which is defined by:

$$L_1(S) = \frac{\sum_{i=1}^{n} \left| S_{SL-based} - S_{grid-based} \right|}{n} \tag{29}$$

where n is the number of grid-blocks and results are normalized with $L_1(S_w)$=0.016 and L_1(T)=1.43. Fig. 7 and Fig. 8 show the impact of NSL and NPU on the norm of difference between predicted water saturation and temperature of the streamline method and those of the grid-based method, respectively. As can be seen, optimal NSL and NPU exist to minimize the norm of difference which in this case these optimum values are NSL=600, NPU=10. It seems that by increasing NPU and NSL the streamline method would become more accurate, but this fact is not generally true. Because, increasing NPU and NSL can lead to the increment of the error caused be mapping parameters between the streamline grid and the 3D underlying grid. Hence, optimum values exist for NSL and NPU to minimize numerical errors.

In addition to the norm of difference for the modified method, this norm is computed for the old method (in which the pressure and conduction equations are solved separately in two different steps instead of solving simultaneously in a coupled system) with NSL=600. Obviously, the modified method could improve the accuracy of streamline method. Furthermore, in some cases the modified method can arise better results compared to the old method, even with fewer NPUs using the same NSLs.

Fig. 7 The impact of the NSL and NPU on the norm of difference between predicted S_w by the modified streamline simulator and the reference case.

Fig. 8 The impact of the NSL and NPU on the norm of difference between predicted temperature by the modified streamline simulator and the reference case.

As previously mentioned, to decrease the error caused by non-linearity effects of viscosity variations, the streamline method has been modified and the conduction equation is solved with the pressure equation at the same time. The effect of this modification on the difference between results of the streamline and the grid-based methods is investigated for different oils and are compared with the old solution method. Four cases for oil viscosity are considered here, such that their maximum viscosity (at 293 K) to minimum viscosity (at 363 K) ratio (VR) changes from 5000 to 10. Fig. 9 illustrates the norm of difference of results for the modified and the old thermal streamline simulator. Results are presented for NPU=10 and NSL=600 and are normalized by $L_1(S_w)$=0.018 and L_1(T)=2.39. As expected, by increasing VR the norm of the difference is growing for both the old and the modified methods. However, the norm of the difference of the modified method, for both S_w and T, is lower than the old method. The difference between these norms is low for small VRs, and by increasing VR their difference becomes higher such that for VR=5000 their results differ about 20%.

Fig. 9 A comparison between norm of difference (relative to the reference case) for the modified and old thermal streamline simulators as a function of VR.

5.2 Hot water injection in a chalk reservoir

The streamline simulator is implemented to investigate the effect of temperature dependency of the relative permeability on oil production. Hence, the streamline-based simulation has been conducted for hot waterflooding in a chalk reservoir, in which the relative permeability is defined by Eq. (25). In addition, in order to scrutinize the effect of variation of the relative permeability with temperature on waterflooding performance, results are compared with those of a reference case using Eq. (24) to define a temperature independent relative permeability function. In this section and the three subsequent ones, hot water is injected at the rate 500 m^3/day into the reservoir.

Comparison of oil production rates of the two mentioned cases is illustrated in Fig. 10. As can be seen, for the temperature independent case after about 200 days, oil production rates in all wells have suddenly declined, while for the temperature dependent case oil production continues with higher rates and declines gradually.

Fig. 11 exhibits the cumulative oil production of the chalk reservoir and the reference one for a time period of 1000 days. It can be seen that the difference between the production volumes of the two compared cases is significant, such that by inclusion of the relative permeability dependency on temperature, after a 1000 days hot waterflooding process, an increase of about 15.4 percent in cumulative oil production of the reservoir has been observed. This difference indicates that ignoring the relative permeability dependency on temperature in chalk reservoirs can cause significant errors in predicted results.

Fig. 10 Comparison of oil production rate in two states when the relative permeability depends or doesn't depend on temperature (chalk reservoir).

Fig. 11 Comparison of cumulative oil production in two states when the relative permeability depends or doesn't depend on temperature (chalk reservoir).

It is interesting to indicate that based on the laboratory studies conducted on core-scale chalk rocks [17], it has been observed that the oil recovery factor of a chalk with variable temperature and consequently a temperature dependent relative permeability can be approximately 12.5% (depending on the injected water temperature and the initial temperature of the reservoir) higher than that of a chalk core in constant temperature (with a temperature independent relative permeability function). The fact that can support the results of this study in a field-scale domain.

5.3 Hot water injection in a limestone reservoir

In this section, the effect of temperature dependency of the relative permeability function on the oil recovery during hot water injection into a limestone reservoir is investigated by using the thermal streamline-based simulator. The temperature dependent relative permeability function of the limestone reservoir is defined by Eq. (26). Similar to the chalk reservoir case, in order to find the effect of variation of the relative permeability versus temperature on the oil production, results of the limestone reservoir are compared with those of the reference case, using Eq. (24) for definition of the relative permeability.

Oil production rates and cumulative oil production of both the limestone and the reference cases are depicted in Fig. 12 and Fig. 13, respectively. As exhibited, oil production rates of wells of the limestone reservoir is more than the chalk reservoir, such that the cumulative oil production of limestone reservoir is approximately 18.1% higher than that of the reference case, for the 1000 days of hot waterflooding process. Especially oil production of Prod-4 is much higher than the other wells of the limestone reservoir, and also the same well of the chalk reservoir.

Fig. 12 Comparison of oil production rate in two states when the relative permeability depends or doesn't depend on temperature (limestone reservoir).

Fig. 13 Comparison of cumulative oil production in two states when the relative permeability depends or doesn't depend on temperature (limestone reservoir).

Therefore, with respect to calculations and the comparison of results obtained from the thermal streamline simulator, it can be concluded that the changes of relative permeability versus temperature will remarkably affect the oil recovery of reservoirs during thermal EOR activities. Hence, it's necessary to consider these variations to study thermal EOR projects.

5.4 Hot water injection in a silica sandstone reservoir

In this section hot waterflooding is simulated in a silica sandstone reservoir. The comparison of oil production rate and cumulative oil production between the temperature dependent and the base cases are shown in Fig. 14 and Fig. 15, respectively. In contrast to the two previous rocks, in the silica sandstone rock the amount of estimated cumulative oil production with temperature dependent relative permeability function, after 1000 days of simulation, is about 22.3% lower than the case with independent relative permeability.

Fig. 14 Comparison of oil production rate in two states when the relative permeability depends or doesn't depend on temperature (silica sandstone reservoir).

Fig. 15 Comparison of cumulative oil production in two states when the relative permeability depends or doesn't depend on temperature (silica sandstone reservoir).

5.5 Hot water injection in an unconsolidated sandstone reservoir

In this part, hot waterflooding in a reservoir with unconsolidated sandstone rocks is simulated. The comparison of oil production rate and cumulative oil production between the base case and the case with temperature dependent relative permeability function are illustrated in Fig. 16 and Fig. 17, respectively. Similar to the silica sandstone reservoir, the estimated oil production will reduce when accounting temperature effects on relative permeability. Such that, after 1000 days of simulation, a gap of about 21.5% can be observed between cumulative oil production of the base and the temperature dependent cases.

Fig. 16 Comparison of oil production rate in two states when the relative permeability depends or doesn't depend on temperature (unconsolidated sandstone reservoir).

Fig. 17 Comparison of cumulative oil production in two states when the relative permeability depends or doesn't depend on temperature (unconsolidated sandstone reservoir).

According to the four investigated reservoir rocks in this section, it can be concluded that the effect of temperature on relative permeability is very important and has to be considered in most of hot waterflooding projects in different reservoir rocks. Eliminating this effect might lead to a large amount of error in numerical simulation predictions during hot water injection process. For limestone and chalk rocks, use of temperature independent relative permeability functions would lead to under-estimation of oil production. But for silica and unconsolidated sandstone rocks, the oil production would be over-estimated, ignoring the impact of temperature on relative permeability.

6. Conclusions

In many thermal enhanced oil recovery projects, relative permeability is considered only a function of saturation, however based on experimental investigations this assumption can lead to large errors in predicted oil recovery. In this paper, two main objectives have been pursued: 1- extension of the streamline-based simulation for simulation of hot water injection process in 3D heavy oil reservoirs considering variations of relative permeability versus temperature; 2- investigation of the effect of temperature dependent relative permeability on oil production of field-scale reservoirs. In order to investigate the problem in more realistic conditions, hot water injection simulations have been performed in a 3D field-scale heterogeneous reservoir model known as SPE-10. Since, in the streamline-based simulation the pressure, the saturation and the energy equations are solved separately, the method might be unable to predict non-linear problems properly. Hence, a new modification has been implemented in the streamline simulation and heat conduction equation has been solved with the pressure equation simultaneously. A sensitivity study has been performed and the modified and the old thermal streamline simulators are compared with each other. Afterward, the impact of relative permeability variations by temperature on the oil recovery has been studied in four types of reservoirs made of chalk, limestone, silica sandstone and unconsolidated sandstone rocks, using the streamline-based simulator. Results revealed that temperature effects on the relative permeability can lead to significant variations in the amount of estimated oil recovery. It has been concluded that ignoring variations of relative permeability against the temperature can cause large errors in predicted results of thermal enhanced oil recovery projects.

References

[1] British Petroleum, Statistical review of world energy June 2014, in, 2014.

[2] M. Siavashi, M.H. Doranehgard, Particle Swarm Optimization of Thermal Enhanced Oil Recovery from Oilfields with Temperature Control, Applied Thermal Engineering, 123 (2017) 658-669.

[3] A. Datta-Gupta, M.J. King, Streamline simulation: theory and practice, Society of Petroleum Engineers, 2007.

[4] R. Batycky, M.J. Blunt, M.R. Thiele, A 3D field-scale streamline-based reservoir simulator, SPE Reservoir Engineering, 12 (1997) 246-254.

[5] V.T. Beraldo, M.J. Blunt, D.J. Schiozer, Compressible streamline-based simulation with changes in oil composition, SPE Reservoir Evaluation & Engineering, 12 (2009) 963-973.

[6] G. Di Donato, M.J. Blunt, Streamline-based dual-porosity simulation of reactive transport and flow in fractured reservoirs, Water Resources Research, 40 (2004) W04203.

[7] M. Ahmadpour, M. Siavashi, M.H. Doranehgard, Numerical simulation of two-phase flow in fractured porous media using streamline simulation and IMPES methods and comparing results with a commercial software, Journal of Central South University, 23 (2016) 2630-2637.

[8] M. Crane, F. Bratvedt, K. Bratvedt, P. Childs, R. Olufsen, A fully compositional streamline simulator, in: SPE Annual Technical Conference and Exhibition, Society of Petroleum Engineers, 2000.

[9] T. Clemens, J. Abdev, M. Thiele, Improved polymer-flood management using streamlines, SPE Reservoir Evaluation & Engineering, 14 (2011) 171-181.

[10] A.M. AlSofi, M.J. Blunt, Streamline-based simulation of non-Newtonian polymer flooding, SPE Journal, 15 (2010) 895-905.

[11] A.M. AlSofi, M.J. Blunt, Polymer flooding design and optimization under economic uncertainty, Journal of Petroleum Science and Engineering, 124 (2014) 46-59.

[12] M. Thiele, R. Batycky, S. Pöllitzer, T. Clemens, Polymer-flood modeling using streamlines, SPE Reservoir Evaluation & Engineering, 13 (2010) 313-322.

[13] M. Siavashi, M.R. Tehrani, A. Nakhaee, Efficient Particle Swarm Optimization of Well Placement to Enhance Oil Recovery Using a Novel Streamline-Based Objective Function, Journal of Energy Resources Technology, 138 (2016) 052903-052903.

[14] U. Pasarai, N. Arihara, A simulator for predicting thermal recovery behavior based on streamline method, in: SPE International Improved Oil Recovery Conference in Asia Pacific, Society of Petroleum Engineers, 2005.

[15] Z. Zhu, M. Gerritsen, M. Thiele, Thermal streamline simulation for hot waterflooding, SPE Reservoir Evaluation & Engineering, 13 (2010) 372-382.

[16] M. Siavashi, M.J. Blunt, M. Raisee, P. Pourafshary, Three-dimensional streamline-based simulation of non-isothermal two-phase flow in heterogeneous porous media, Computers & Fluids, 103 (2014) 116-131.

[17] A.A. Hamouda, O. Karoussi, Effect of temperature, wettability and relative permeability on oil recovery from oil-wet chalk, Energies, 1 (2008) 19-34.

[18] M. Akhlaghinia, F. Torabi, C.W. Chan, Effect of Temperature on Two-Phase Relative Permeabilities of Heavy Oil, Water, Carbon Dioxide, and Methane Determined by Displacement Technique, Energy & Fuels, 27 (2013) 1185-1193.

[19] M. Akhlaghinia, F. Torabi, C.W. Chan, Experimental investigation of temperature effect on three-phase relative permeability isoperms in heavy oil systems, Fuel, 118 (2014) 281-290.

[20] A. Hamouda, O. Karoussi, E. Chukwudeme, Relative permeability as a function of temperature, initial water saturation and flooding fluid compositions for modified oil-wet chalk, Journal of Petroleum Science and Engineering, 63 (2008) 61-72.

[21] B.S. Sola, F. Rashidi, T. Babadagli, Temperature effects on the heavy oil/water relative permeabilities of carbonate rocks, Journal of Petroleum Science and Engineering, 59 (2007) 27-42.

[22] S. Akin, L.M. Castanier, W.E. Brigham, Effect of temperature on heavy-oil/water relative permeabilities, in: SPE Annual Technical Conference and Exhibition, Society of Petroleum Engineers, 1998.

[23] K. Nakornthap, R.D. Evans, Temperature-dependent relative permeability and its effect on oil displacement by thermal methods, SPE Reservoir Engineering, 1.03 (1986) 230-242.

[24] J.M. Schembre, G.-Q. Tang, A.R. Kovscek, Interrelationship of Temperature and Wettability on the Relative Permeability of Heavy Oil in Diatomaceous Rocks (includes associated discussion and reply), SPE Reservoir Evaluation & Engineering, 9 (2006) 239-250.

[25] P. Shen, B. Zhu, X.-B. Li, Y.-S. Wu, The Influence of Interfacial Tension on Water-Oil Two-Phase Relative Permeability, in: SPE/DOE Symposium on Improved Oil Recovery, Society of Petroleum Engineers, 2006.

[26] Z. Chen, G. Huan, Y. Ma, Computational methods for multiphase flows in porous media, Siam, Unitided States, 2006.

[27] E. Abreu, D. Conceição, Numerical modeling of degenerate equations in porous media flow, Journal of Scientific Computing, 55 (2013) 688-717.

[28] D.W. Pollock, Semianalytical computation of path lines for finite-difference models, Groundwater, 26 (1988) 743-750.

[29] M. Siavashi, P. Pourafshary, M. Raisee, Application of space–time conservation element and solution element method in streamline simulation, Journal of Petroleum Science and Engineering, 96 (2012) 58-67.

[30] R. Courant, K. Friedrichs, H. Lewy, On the partial difference equations of mathematical physics, IBM Journal of Research and Development, 11 (1967) 215-234.

[31] Y. Liu, S. Shi, Y. Wang, J. Xie, G. Xie, A new model for predicting the viscosity of heavy oil, Petroleum Science and Technology, 34 (2016) 832-837.

[32] B.E. Poling, John M. Prausnitz, and John P. O'connell, The properties of gases and liquids, McGraw-Hill, New York, 2001.

[33] O. Alomair, M. Jumaa, A. Alkoriem, M. Hamed, Heavy oil viscosity and density prediction at normal and elevated temperatures, Journal of Petroleum Exploration and Production Technology, 6 (2015) 253-263.

[34] B.E. Poling, J.M. Prausnitz, J.P. O'connell, The properties of gases and liquids, McGraw-Hill New York, 2001.

[35] W.H. Somerton, Thermal properties and temperature-related behavior of rock/fluid systems, Elsevier, 1992.

[36] Y. Cengel, M. Boles, Fundamentals of Thermodynamics, in, New York: Mc-Graw-Hill, 2002.

[37] R.E. Sonntag, C. Borgnakke, G.J. Van Wylen, S. Van Wyk, Fundamentals of thermodynamics, Wiley New York, 2002.

[38] S.W. Poston, et at., The effect of temperature on irreducible water saturation and relative permeability of unconsolidated sands, Society of Petroleum Engineers Journal, 10 (1970) 171-180.

[39] B.B. Maini, T. Okazawa, Effects of temperature on heavy oil-water relative permeability of sand, Journal of Canadian Petroleum Technology, 26 (1987) 2118-2128.

[40] H.S. Al-Hadhrami, M.J. Blunt, Thermally induced wettability alteration to improve oil recovery in fractured reservoirs, in: SPE/DOE Improved Oil Recovery Symposium, Society of Petroleum Engineers, 2000.

[41] A.A. Hamouda, K.A. Rezaei Gomari, Influence of temperature on wettability alteration of carbonate reservoirs, in: SPE/DOE Symposium on Improved Oil Recovery, Society of Petroleum Engineers, 2006.

[42] P. Bhambri, K. Mohanty, Two-and three-hydrocarbon phase streamline-based compositional simulation of gas injections, Journal of Petroleum Science and Engineering, 62 (2008) 16-27.

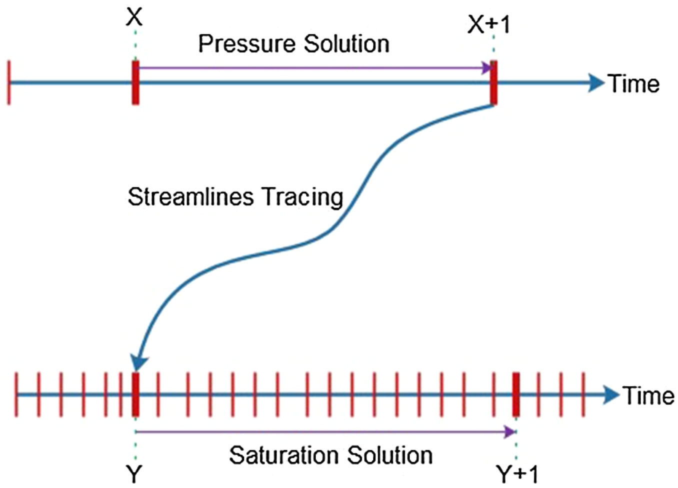
X
Pressure Solution
X+1
Time
Streamlines Tracing
Time
Y
Saturation Solution
Y+1

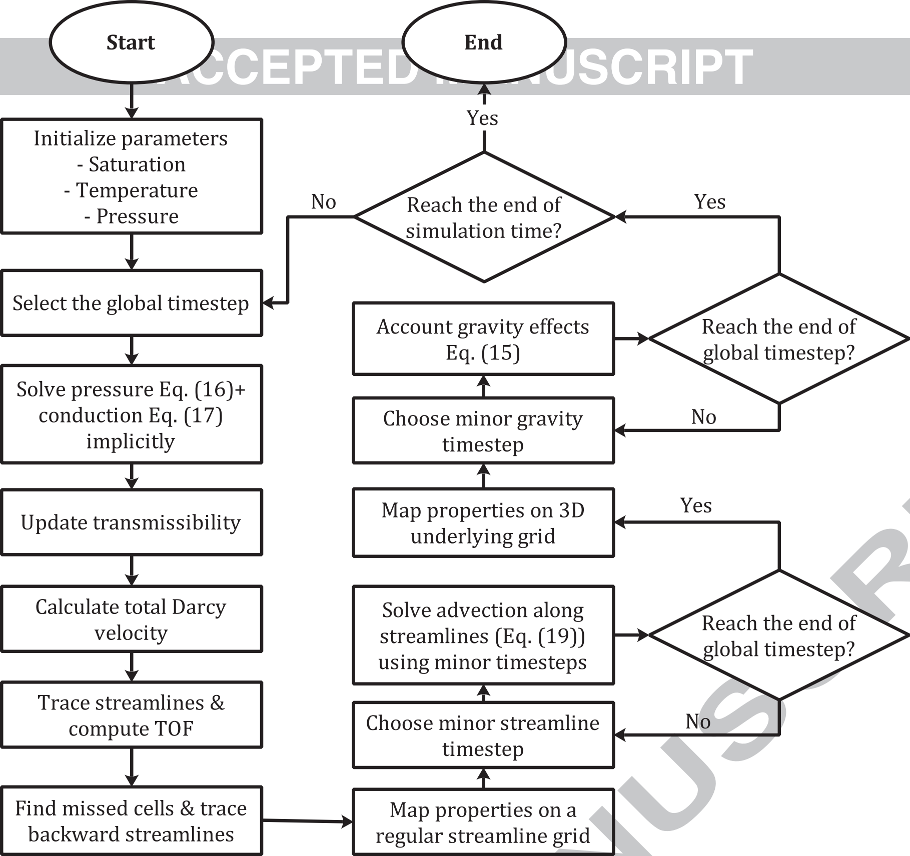
Start
Initialize parameters
- Saturation
- Temperature
- Pressure
Select the global timestep
Solve pressure Eq. (16)+ conduction Eq. (17) implicitly
Update transmissibility
Calculate total Darcy velocity
Trace streamlines & compute TOF
Find missed cells & trace backward streamlines
Map properties on a regular streamline grid
Choose minor streamline timestep
Solve advection along streamlines (Eq. (19)) using minor timesteps
Reach the end of global timestep?
No
Yes
Map properties on 3D underlying grid
Choose minor gravity timestep
Account gravity effects Eq. (15)
Reach the end of global timestep?
No
Yes
Reach the end of simulation time?
No
Yes
End

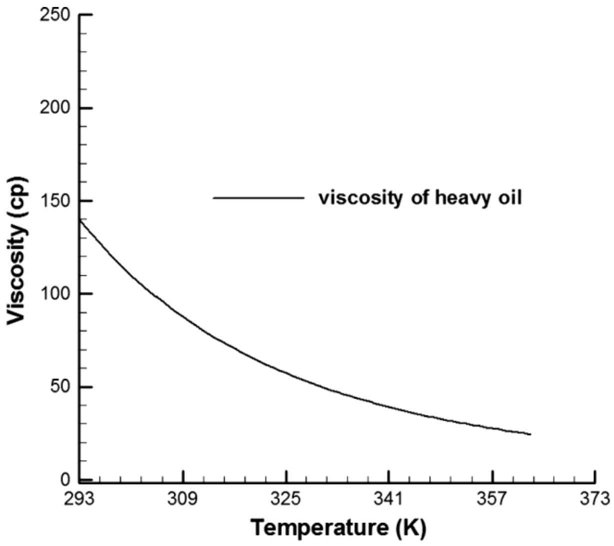

250
200
150
100
50
0
Viscosity (cp)
viscosity of heavy oil
293
309
325
341
357
373
Temperature (K)

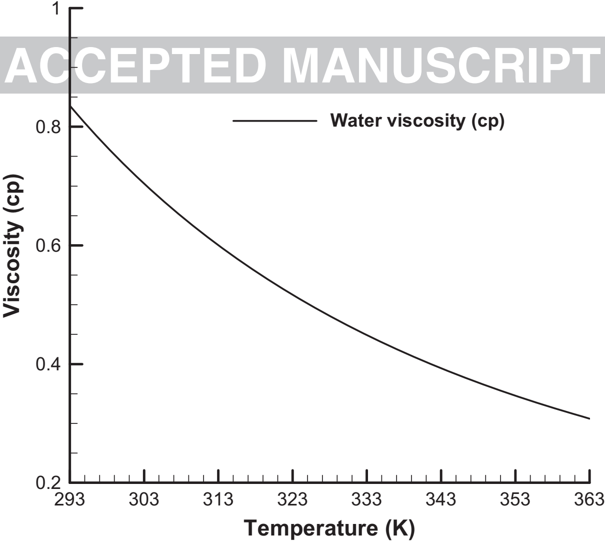
Water viscosity (cp)
Viscosity (cp)
Temperature (K)
1
0.8
0.6
0.4
0.2
293
303
313
323
333
343
353
363

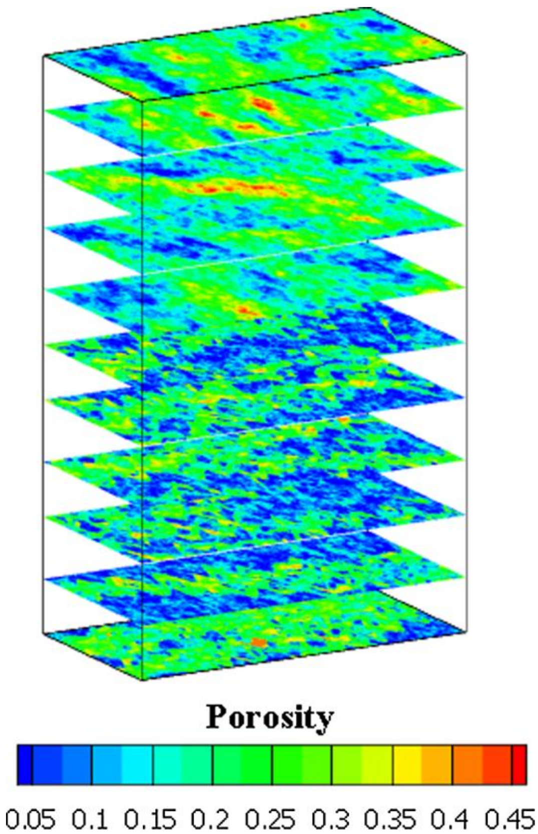
Porosity
0.05 0.1 0.15 0.2 0.25 0.3 0.35 0.4 0.45

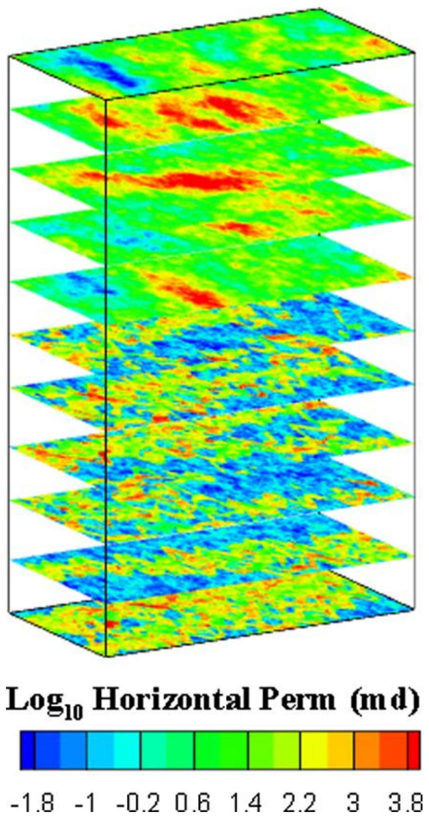
Log10 Horizontal Perm (md)
-1.8 -1 -0.2 0.6 1.4 2.2 3 3.8

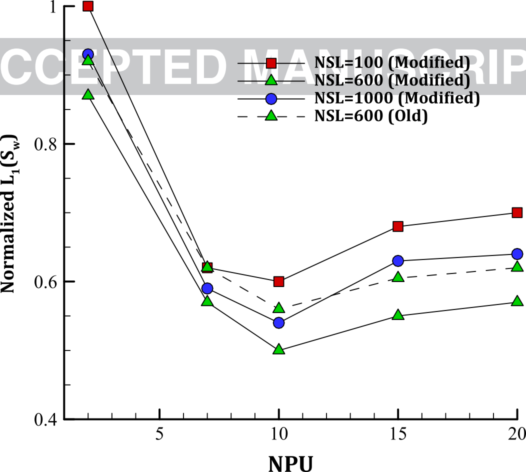

NSL=100 (Modified)
NSL=600 (Modified)
NSL=1000 (Modified)
NSL=600 (Old)
Normalized $L_1(S_w)$
NPU
1
0.8
0.6
0.4
5
10
15
20

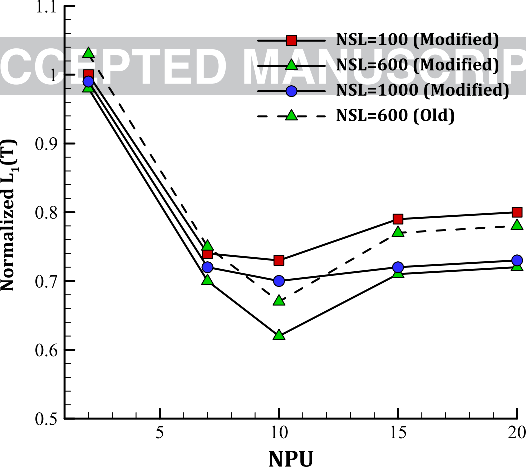

NSL=100 (Modified)
NSL=600 (Modified)
NSL=1000 (Modified)
NSL=600 (Old)
Normalized L_1(T)
NPU
1.1
1
0.9
0.8
0.7
0.6
0.5
5
10
15
20

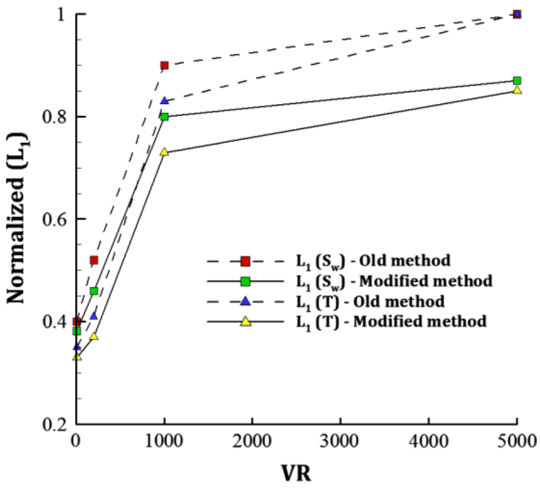
Normalized (L_1)
1
0.8
0.6
0.4
0.2
0
1000
2000
3000
4000
5000
VR
L_1 (S_w) - Old method
L_1 (S_w) - Modified method
L_1 (T) - Old method
L_1 (T) - Modified method

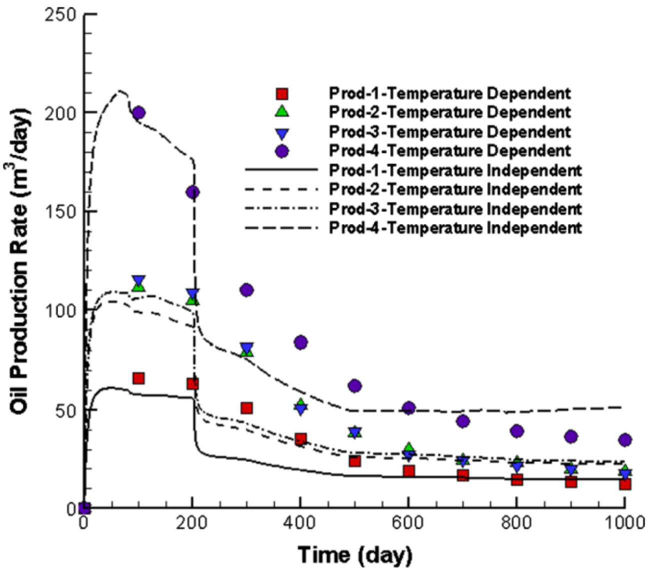

Oil Production Rate (m³/day)
Time (day)
Prod-1-Temperature Dependent
Prod-2-Temperature Dependent
Prod-3-Temperature Dependent
Prod-4-Temperature Dependent
Prod-1-Temperature Independent
Prod-2-Temperature Independent
Prod-3-Temperature Independent
Prod-4-Temperature Independent
0
50
100
150
200
250
0
200
400
600
800
1000

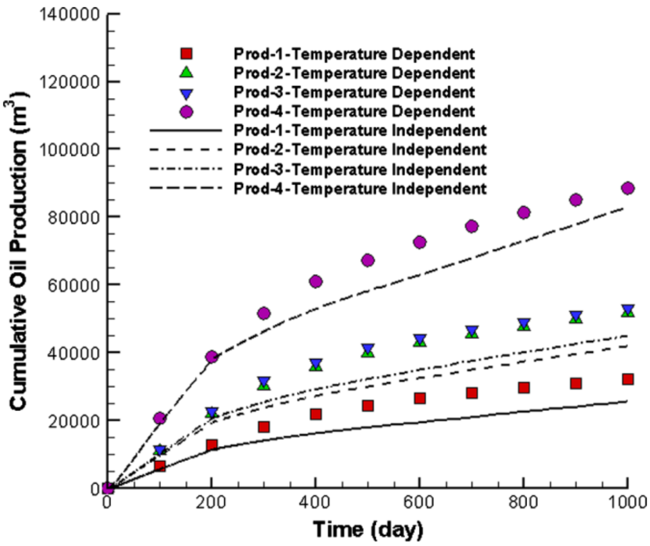
Prod-1-Temperature Dependent
Prod-2-Temperature Dependent
Prod-3-Temperature Dependent
Prod-4-Temperature Dependent
Prod-1-Temperature Independent
Prod-2-Temperature Independent
Prod-3-Temperature Independent
Prod-4-Temperature Independent
Cumulative Oil Production (m3)
Time (day)
0
20000
40000
60000
80000
100000
120000
140000
0
200
400
600
800
1000

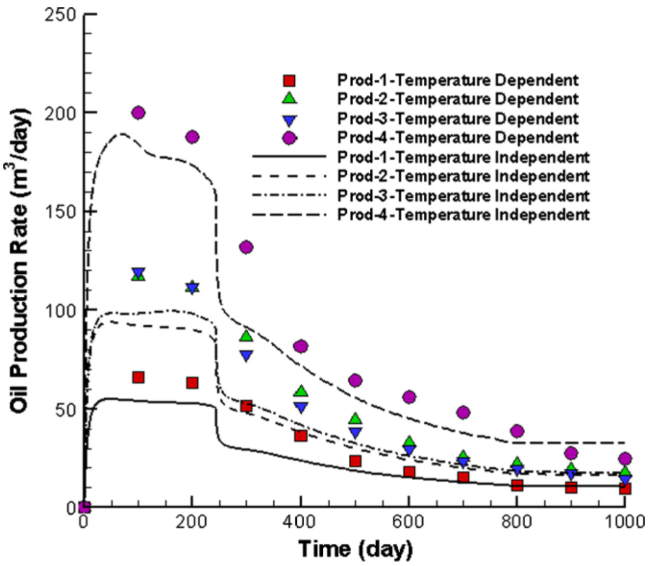

250
200
150
100
50
0
Oil Production Rate (m^3/day)
0
200
400
600
800
1000
Time (day)
Prod-1-Temperature Dependent
Prod-2-Temperature Dependent
Prod-3-Temperature Dependent
Prod-4-Temperature Dependent
Prod-1-Temperature Independent
Prod-2-Temperature Independent
Prod-3-Temperature Independent
Prod-4-Temperature Independent

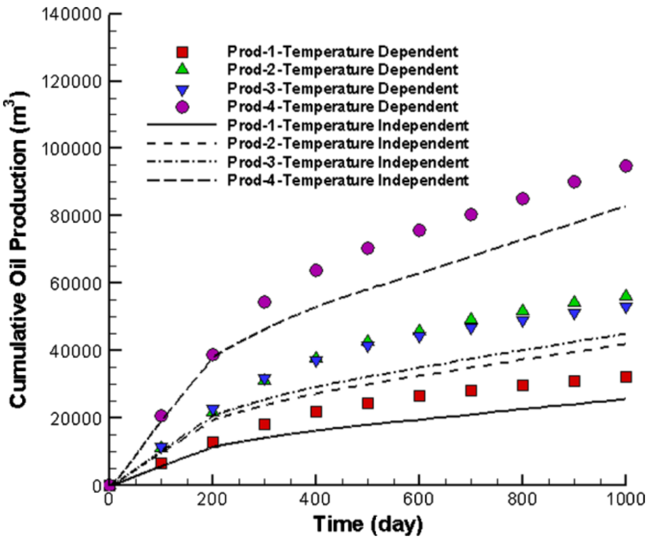

140000
120000
100000
80000
60000
40000
20000
0
Cumulative Oil Production (m^3)
0
200
400
600
800
1000
Time (day)
Prod-1-Temperature Dependent
Prod-2-Temperature Dependent
Prod-3-Temperature Dependent
Prod-4-Temperature Dependent
Prod-1-Temperature Independent
Prod-2-Temperature Independent
Prod-3-Temperature Independent
Prod-4-Temperature Independent

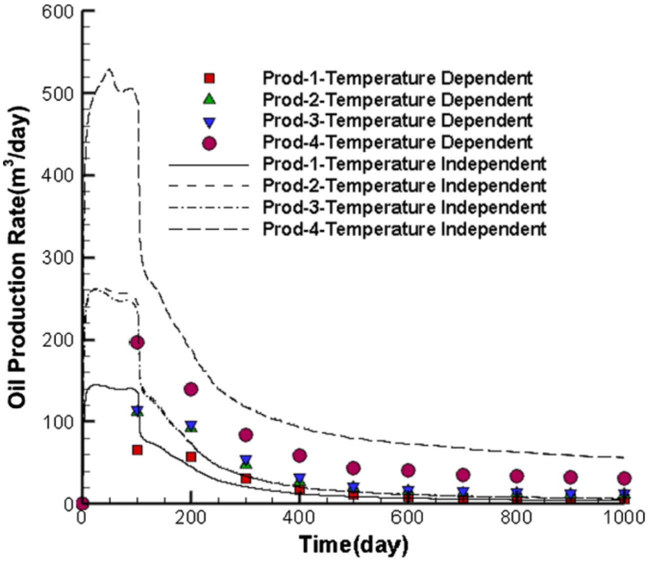

Prod-1-Temperature Dependent
Prod-2-Temperature Dependent
Prod-3-Temperature Dependent
Prod-4-Temperature Dependent
Prod-1-Temperature Independent
Prod-2-Temperature Independent
Prod-3-Temperature Independent
Prod-4-Temperature Independent
Oil Production Rate(m^3/day)
Time(day)
0
100
200
300
400
500
600
800
1000

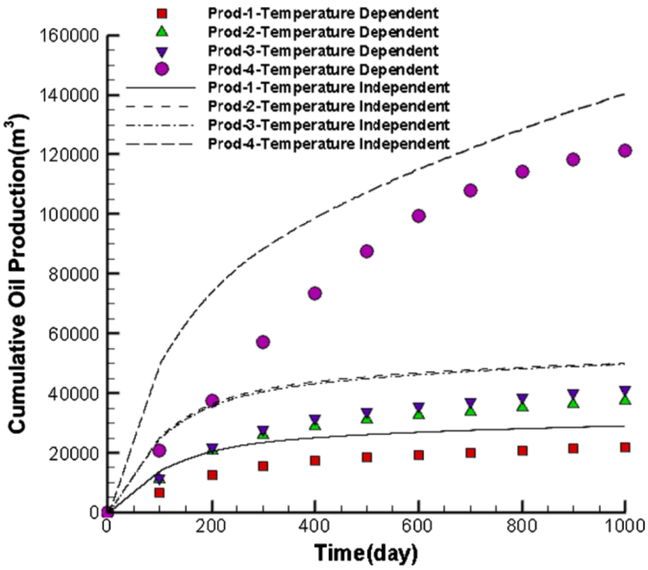
Prod-1-Temperature Dependent
Prod-2-Temperature Dependent
Prod-3-Temperature Dependent
Prod-4-Temperature Dependent
Prod-1-Temperature Independent
Prod-2-Temperature Independent
Prod-3-Temperature Independent
Prod-4-Temperature Independent
Cumulative Oil Production(m3)
Time(day)
0
20000
40000
60000
80000
100000
120000
140000
160000
0
200
400
600
800
1000

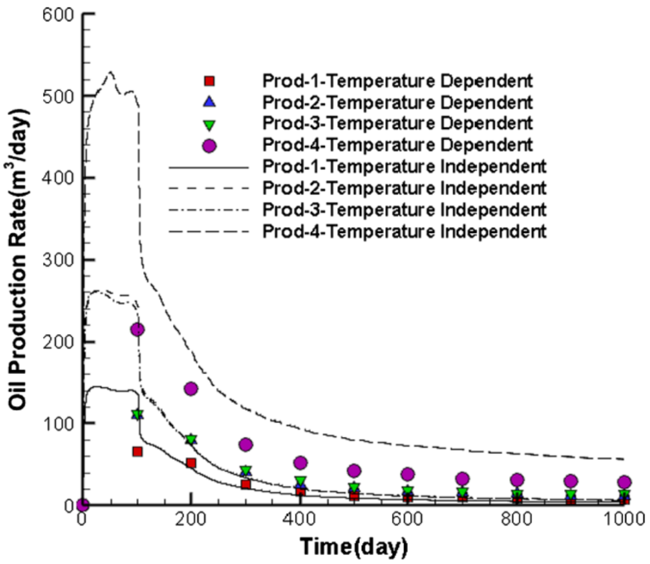

Prod-1-Temperature Dependent
Prod-2-Temperature Dependent
Prod-3-Temperature Dependent
Prod-4-Temperature Dependent
Prod-1-Temperature Independent
Prod-2-Temperature Independent
Prod-3-Temperature Independent
Prod-4-Temperature Independent
Oil Production Rate(m3/day)
Time(day)
0
100
200
300
400
500
600
800
1000

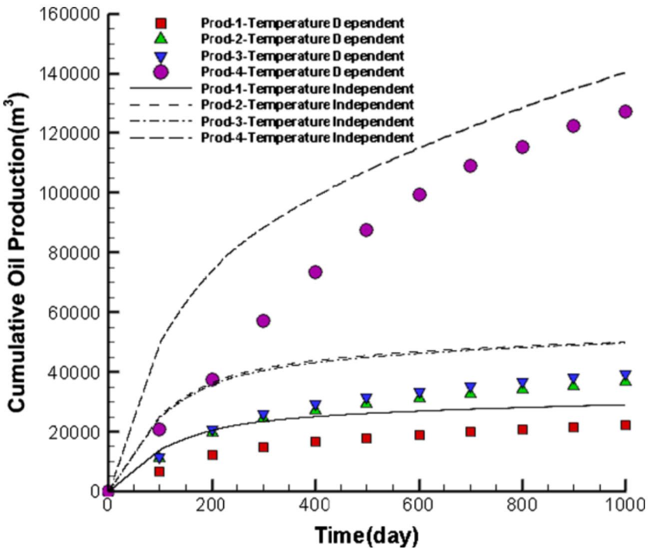
Prod-1-Temperature Dependent
Prod-2-Temperature Dependent
Prod-3-Temperature Dependent
Prod-4-Temperature Dependent
Prod-1-Temperature Independent
Prod-2-Temperature Independent
Prod-3-Temperature Independent
Prod-4-Temperature Independent
Cumulative Oil Production(m^3)
Time(day)
0
20000
40000
60000
80000
100000
120000
140000
160000
0
200
400
600
800
1000

Highlights

- Hot water injection is simulated in 3D heavy oilfields using streamline approach
- Relative permeability and viscosity of oil strongly depends on temperature
- Streamline method is improved to better handle the high non-linearity of equations
- The improved numerical method is accurate with excellent performance
- Variation of relative permeability with temperature has a high impact on COP